



PLANT SCIENCES

The causal mutation leading to sweetness in modern white lupin cultivars

Davide Mancinotti¹, Katarzyna Czepiel², Jemma L. Taylor³, Hajar Golshadi Galehshahi¹, Lillian A. Møller⁴, Mikkel K. Jensen⁴, Mohammed Saddik Motawia¹, Bárbara Hufnagel^{5†}, Alexandre Soriano^{5†}, Likawent Yeheyis⁶, Louise Kjaerulff⁷, Benjamin Péret⁵, Dan Staerk⁷, Toni Wendt⁴, Matthew N. Nelson^{3,8,9}, Magdalena Kroc², Fernando Geu-Flores^{1*}

Copyright © 2023 The Authors, some rights reserved; exclusive licensee American Association for the Advancement of Science. No claim to original U.S. Government Works. Distributed under a Creative Commons Attribution License 4.0 (CC BY).

Lupins are high-protein crops that are rapidly gaining interest as hardy alternatives to soybean; however, they accumulate antinutritional alkaloids of the quinolizidine type (QAs). Lupin domestication was enabled by the discovery of genetic loci conferring low QA levels (sweetness), but the precise identity of the underlying genes remains uncertain. We show that *pauper*, the most common sweet locus in white lupin, encodes an acetyltransferase (AT) unexpectedly involved in the early QA pathway. In *pauper* plants, a single-nucleotide polymorphism (SNP) strongly impairs AT activity, causing pathway blockage. We corroborate our hypothesis by replicating the *pauper* phenotype in narrow-leaved lupin via mutagenesis. Our work adds a new dimension to QA biosynthesis and establishes the identity of a lupin sweet gene for the first time, thus facilitating lupin breeding and enabling domestication of other QA-containing legumes.

INTRODUCTION

In the last decade, European efforts to diversify the local production of protein crops have intensified. Among the drivers are the impending shift toward plant protein-rich diets (1) and the awareness of the environmental impact of soybean cultivation and import (2). Lupins (*Lupinus* spp.) are the only protein crops whose seed protein content (up to 44%) can rival that of soybean (3). Moreover, lupins are relatively more tolerant to several abiotic stresses than other legumes and have great potential for the recovery of poor soils (3). However, lupin seeds naturally accumulate bitter and toxic alkaloids of the quinolizidine type (QAs) (4). The modern domestication of lupins began in the 1930s with the identification of low QA ("sweet") lines whose seeds could be consumed directly without debittering (5). Starting in the 1960s, the addition of agronomic traits such as loss of seed dispersal and early flowering enabled the expansion of sweet lupin cultivation (6). Now, the two most widely cultivated species are white lupin (*Lupinus albus*) and narrow-leaved lupin (*Lupinus angustifolius*). Their respective centers of diversity lie in the Mediterranean basin (7, 8) and the cultivation of sweet varieties now extends to a range of European and African countries as well as Australia and Chile. In Ethiopia, the severe shortage of protein for animal feed has sparked recent

efforts to develop sweet white lupin cultivars adapted to local climates (9).

A few individual loci conferring sweetness exist; however, the precise identity of the underlying genes remains uncertain. QAs are known to be synthesized in green tissues and transported to the seed (10), but the QA pathway remains largely unknown (Fig. 1A). Of the hypothetical six to nine biosynthetic enzymes (11), only the first two are known: lysine decarboxylase (LDC) (12) and copper amine oxidase (CAO) (13) (Fig. 1A). Because the known sweet loci confer sweetness in both seeds and green tissues, uncovering the underlying genes will not only aid trait introgression but also help uncover the QA pathway. In white lupin (*L. albus* L.), the most widely exploited sweet locus is *pauper*, which lowers seed QA content down to 0.02 to 0.05% dry seed weight (14). The first molecular marker for *pauper* was published in 2008 and lay at a genetic distance of 1.8 cM (15). Recently, the sequencing of the white lupin genome allowed the mapping of *pauper* to a 958-kb region containing 66 protein-coding genes on chromosome 18 (16). Among the transcription factors, transport proteins, and enzymes encoded within this region, a gene encoding a predicted BAHD acyltransferase, *AT* (Lalb_Chr18g0051511), was identified as a strong candidate for *pauper* (17). The best current marker for *pauper* is located in the coding sequence of *AT* (18, 19). However, this marker does not appear to be a perfect predictor of sweetness, suggesting that *AT* might not be the *pauper* gene (18, 20).

AT was first identified together with *LDC* and *CAO* in a differential expression screen between bitter and sweet narrow-leaved lupin (*L. angustifolius* L.) varieties (21). *LDC* and *CAO* were assigned to the first two steps of the pathway (Fig. 1A), and their activities were later confirmed biochemically (12, 13, 22). By contrast, *AT* was putatively assigned to the synthesis of QA esters in the terminal part of the pathway (21), but its activity has not been verified. Evidence in support of a more central role for *AT* comes from the fact that the gene is coregulated with *LDC* and *CAO*, while the synthesis of QA esters appears to be decoupled from the core of the pathway (10, 23). Nevertheless, none of the published biosynthetic

¹Section for Plant Biochemistry and Copenhagen Plant Science Centre, Department of Plant and Environmental Sciences, University of Copenhagen, Thorvaldsensvej 40, 1871 Frederiksberg, Denmark. ²Legume Genomics Team, Institute of Plant Genetics, Polish Academy of Sciences, Strzeszyńska 34, Poznań, Poland. ³Royal Botanic Gardens Kew, Wakehurst Place, Ardingly, West Sussex RH17 6TN, UK. ⁴Traitomic A/S, J.C. Jacobsens Gade 14, 1799 Copenhagen, Denmark. ⁵IPSiM, University of Montpellier, CNRS, INRAE, Institut Agro, Montpellier, France. ⁶Amhara Agricultural Research Institute, Bahir Dar, Ethiopia. ⁷Department of Drug Design and Pharmacology, University of Copenhagen, Universitetsparken 2, 2100 Copenhagen, Denmark. ⁸Agriculture and Food, Commonwealth Scientific and Industrial Research Organisation, Floreat, WA 6014, Australia. ⁹The UWA Institute of Agriculture, The University of Western Australia, 35 Stirling Highway, Perth, WA 6009, Australia.

*Corresponding author. Email: feg@plen.ku.dk

†Present address: UMR AGAP Institut, University of Montpellier, CIRAD, INRAE, Institut Agro, Montpellier, France.

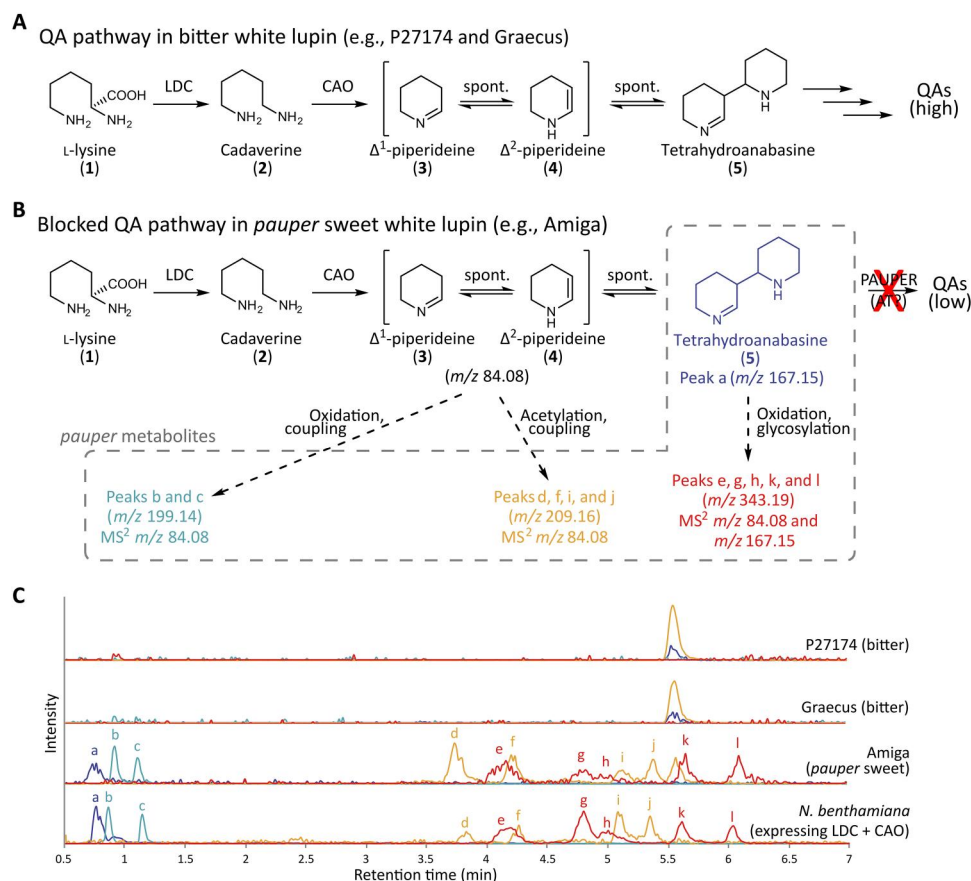


Fig. 1. The distinctive chemotype of sweet white lupins of the *pauper* type. (A) Early QA biosynthesis pathway in bitter lupins according to the prevalent pathway hypothesis. spont.: spontaneous reaction. (B) Proposed QA pathway blockage accounting for sweetness in *pauper* white lupin. Distinctive metabolites accumulate in *pauper* plants (*pauper* metabolites), suggesting that the blockage occurs just downstream of the step catalyzed by CAO. Dashed arrows show the formation of *pauper* metabolites upon accumulation of the immediate product of CAO (Δ^1 -piperidine, **3**) and its spontaneously formed dimer (tetrahydroanabasine, **5**). The origin of the *pauper* metabolites was inferred from their MS^2 spectra (fig. S1), particularly from the presence of fragments of m/z 84.08 (corresponding to Δ^1 -piperidine, **3**) and m/z 167.15 (corresponding to tetrahydroanabasine, **5**). (C) Representative LC-MS chromatograms of leaf extracts from two bitter (P27174, Graecus) and one *pauper* sweet (Amiga) white lupin lines (top three chromatograms) as well as an extract of *N. benthamiana* leaves transiently expressing LDC and CAO (bottom chromatogram). Accumulation of *pauper* metabolites is observed in the leaves of *N. benthamiana* upon transient coexpression of LDC and CAO. Traces are extracted ion chromatograms (EICs) of the most representative *pauper* metabolites (mean $m/z \pm 0.01$). Signal intensities were adjusted to aid visualization (see Materials and Methods for scaling factors).

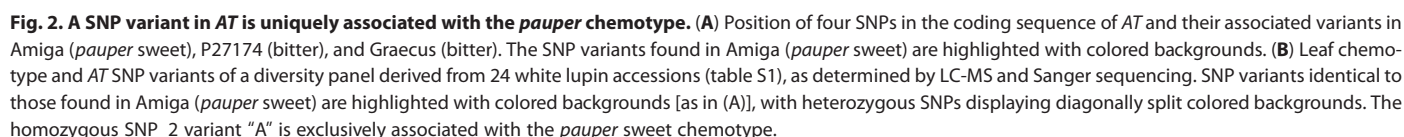
hypotheses predict any acylation at the core of the QA pathway (11), so it is unclear which role *AT* might play there. Intrigued by the conflicting evidence and the prospect of uncovering a novel facet of QA biosynthesis, we decided to investigate whether *AT* really is the *pauper* gene in white lupin.

RESULTS AND DISCUSSION

Plants bearing the *pauper* allele do not show reduced expression levels of *LDC* and *CAO* compared to bitter plants (16), suggesting that the whole pathway is not suppressed. We speculated that the sweetness in *pauper* plants might be due to pathway blockage, which could leave a metabolic footprint in biosynthetic tissues. Thus, we carried out a liquid chromatography–mass spectrometry (LC-MS)–based untargeted metabolite analysis of three white lupin lines: the wild accession Graecus (bitter), the Ethiopian landrace P27174 (bitter), and the modern *pauper* cultivar Amiga (sweet). For the analysis, we chose two types of biosynthetic tissues, leaves

and stems. We identified 12 compounds that were present in most samples of Amiga but were absent from the corresponding P27174 and Graecus samples (Fig. 1B and fig. S1). Six of the compounds (Fig. 1B, cyan and orange traces) appeared to be derivatives of the product of CAO (Δ^1 -piperidine, **3**) based on their MS^2 spectra [fig. S1; MS^2 fragment of mass/charge ratio (m/z) 84]. The other six compounds (Fig. 1B, blue and red traces) appeared to be either tetrahydroanabasine (**5**)—the spontaneous dimerization product of Δ^1 -piperidine (**3**)—or derivatives thereof (fig. S1; MS^2 fragment of m/z 167). Overall, the metabolite data suggest that the biosynthesis of QAs is blocked in *pauper* plants at a step immediately downstream of CAO, leading to the accumulation of QA pathway intermediates and their derivatives (“*pauper* metabolites”; Fig. 1B). To further explore this hypothesis, we attempted to reconstruct a similarly blocked QA pathway in planta by transiently coexpressing LDC and CAO in the leaves of *Nicotiana benthamiana*, which does not naturally produce QAs. As predicted, we were

We functionally characterized AT *in vivo* by transiently expressing the version from P27174 in the leaves of *N. benthamiana* together with LDC and CAO. We found that one compound accumulated in large amounts and appeared to be a monoacetylated derivative of tetrahydroanabasine (**5**) (neutral loss of 42 Da giving a fragment of *m/z* 167 in MS²) (Fig. 3A). We purified the compound and elucidated its structure by nuclear magnetic resonance (NMR) spectroscopy (figs. S3 to S8), which identified it as the bipiperidine alkaloid ammodendrine (**6**) (Fig. 3A and fig. S3). It has long been known that ammodendrine (**6**) derives from cadaverine (24) and that it occurs in many species that also produce QAs (25). However, to the best of our knowledge, ammodendrine (**6**) has not been proposed as an intermediate in the biosynthesis of QAs. The vast majority of QAs are not *N*-acetylated, which implies that the acetyl group added by AT would have to be removed at a later step in the core QA pathway. Acetylation and subsequent deacetylation are not unprecedented in



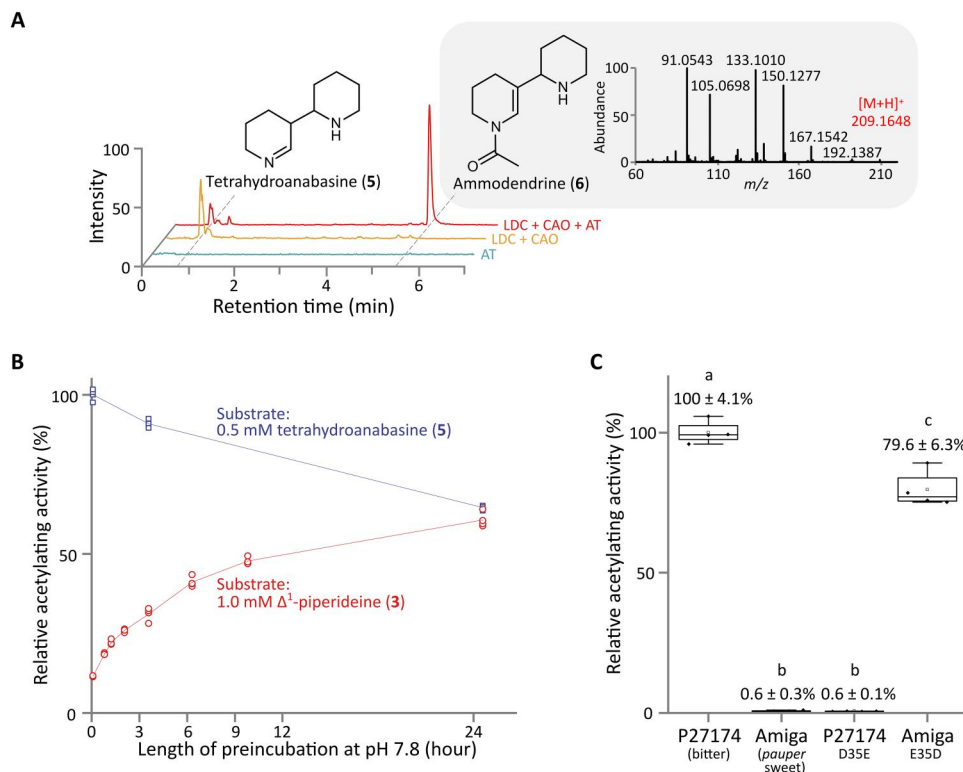


Fig. 3. A single SNP in AT leads to strongly impaired AT enzyme activity. (A) Representative LC-MS chromatograms of extracts from leaves of *N. benthamiana* expressing LDC, CAO, and AT (P27174 bitter version) in different combinations, showing the accumulation of ammodendrine (6) and its precursor, tetrahydroanabasine (5). MS² spectrum (22.9 eV) of ammodendrine (6) is also shown (light gray box). Traces are combined EICs of *m/z* 167.15 ± 0.01 and *m/z* 209.16 ± 0.01. (B) In vitro acetylating activity of AT (P27174 bitter version) against the Δ¹-piperidine monomer (3) and its dimer (tetrahydroanabasine, 5), showing strong preference for the latter. Monomer and dimer solutions were incubated at pH 7.8 for up to 24 hours before initiating the assay to probe the equilibrium between (3) and (5) at near-physiological pH. Lines connect the mean relative activities at each time point (*n* = 4). (C) In vitro acetylating activity of different versions of AT against tetrahydroanabasine (5) showing the effect of the *pauper* variant at SNP_2. In the box plots, the center line represents the median, the box limits represent the upper and lower quartiles, and the whiskers represent maximum and minimum values. Data labels are mean activities relative to P27174 (bitter version) ± 95% confidence interval (*n* = 4). Letters indicate significant differences [one-way analysis of variance (ANOVA) with Tukey's post hoc test, *P* < 0.05].

alkaloid biosynthesis, for example, in the biosynthesis of benzylisoquinoline (26) and monoterpene indole alkaloids (27, 28). If acetylation occurs in the early QA pathway, the current biosynthetic pathway proposal (11) needs to be amended.

We then developed an absorbance-based assay in microtiter plate format to analyze the AT reaction. We fused the P27174 version of AT to maltose-binding protein (MBP) to improve the solubility of the enzyme (fig. S2A), which enabled expression in *Escherichia coli* and subsequent purification (fig. S2, B to E). Purified MBP-AT was assayed separately against the product of CAO, Δ¹-piperidine (3), and its spontaneously formed dimer, tetrahydroanabasine (5). The initial reaction rate was eightfold higher with tetrahydroanabasine (5) compared to Δ¹-piperidine (3) (Fig. 3B), suggesting that the dimer is the physiological substrate. Assays with the Amiga version of AT showed a notable impairment in activity down to 0.6% of the P27174 version (Fig. 3C). We then probed the impact of SNP_2 on activity. We observed that introducing the Amiga variant of SNP_2 into P27174 was sufficient to bring the activity of the enzyme down to the same level as the Amiga version itself (Fig. 3C). Conversely, we could rescue most of the activity of the Amiga version by solely exchanging its SNP_2 variant with the one from P27174 (Fig. 3C), which agrees with the results of our

diversity panel screens (Fig. 2B and table S2). In Amiga, SNP_2 causes the conservative mutation Asp³⁵Glu (Fig. 2A). Asp³⁵ is highly conserved in BAHD acyltransferases, and a mutagenesis study in vinorine synthase from *Rauvolfia serpentina* showed a comparable reduction in activity upon exchange with Ala (29). Together, our biochemical and genetic results strongly suggest that SNP_2 is indeed the *pauper* mutation.

To confirm the physiological role of AT, we built a large mutant library of a bitter cultivar of the related species narrow-leaved lupin. For library construction, we treated around 100,000 seeds (15 kg) with a low dose of mutagen [0.1% ethyl methanesulfonate (EMS)] to minimize the frequency of off-target mutations. We then used FIND-IT technology (30) to isolate an early stop codon mutant in the AT gene (AT^{KO}, TGG to TAG at codon 169) (Fig. 4A). The original heterozygous plant did not show a metabolic phenotype (Fig. 4B, upper and middle chromatograms). However, its homozygous mutant progeny displayed foliar sweetness (Fig. 4B, lower chromatogram) and accumulation of *pauper* metabolites (which were undetectable in leaves of the parent bitter cultivar) (Fig. 4C). The *pauper*-like leaf phenotype is consistent with the loss of AT activity at the proposed biosynthetic step (Fig. 1B). Seeds from homozygous mutant plants were also sweet, with a 110-fold reduction in

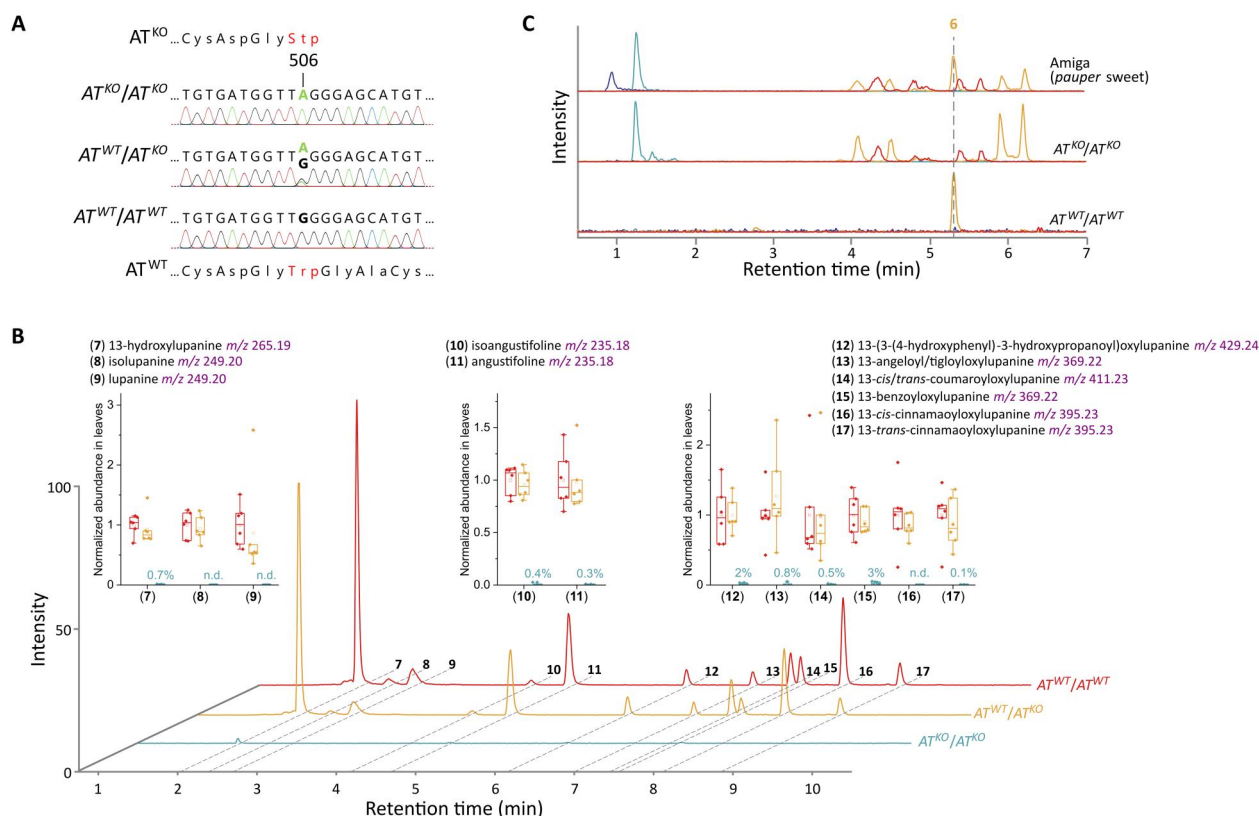


Fig. 4. Inactivation of the AT gene in narrow-leaved lupin leads to pauper-like sweetness. (A) Genotyping of mutagenized narrow-leaved lupin plants carrying the wild-type AT allele (AT^{WT}) or an early stop codon allele (AT^{KO}). (B) Distribution and abundance of 11 major QAs (7 to 17) in the leaves of narrow-leaved lupin carrying the AT^{WT} and AT^{KO} alleles. Traces are combined EICs of *m/z* 235.18 ± 0.01, *m/z* 249.20 ± 0.01, *m/z* 265.19 ± 0.01, *m/z* 347.23 ± 0.01, *m/z* 369.22 ± 0.01, *m/z* 395.23 ± 0.01, *m/z* 411.23 ± 0.01, and *m/z* 429.24 ± 0.01. In the box plots, the center line represents the median, the box limits represent the upper and lower quartiles, and the whiskers represent maximum and minimum values. Data labels represent the relative abundance (%) in homozygous AT^{KO} plants relative to homozygous AT^{WT} plants (*n* = 6). n.d., not detected at the working dilution. (C) Representative LC-MS chromatograms showing the accumulation of pauper metabolites and the absence of ammodendrine (6) in homozygous AT^{KO} plants. EIC traces correspond to *m/z* 167.15 ± 0.01 (blue), *m/z* 199.14 ± 0.01 (cyan), *m/z* 209.16 ± 0.01 (orange), and *m/z* 343.19 ± 0.01 (red).

QA levels compared to seeds from wild-type sibling plants (0.028% compared to 3.07% dry seed weight) (table S4). These low QA levels are within the range of pauper white lupin cultivars (0.02 to 0.05%) (14), confirming that AT is an attractive target for the domestication of lupins and other QA-containing legumes. In narrow-leaved lupin, AT constitutes a novel sweet gene distinct from the universally used *iucundus* (31, 32) and conferring comparable sweetness (33) (table S4). Under growth chamber conditions, the homozygous AT^{KO} mutant displayed no noticeable phenotype. Originating from chemical mutagenesis, the mutant is exempted from Europe's strict policy on genetically modified organisms (GMOs) and thus can enter breeding programs without introducing regulatory hurdles.

The discovery of acetylation in early QA biosynthesis has led us to re-examine the current QA pathway hypothesis (11). Two theoretical challenges arose during this re-examination. First, our in vitro studies suggested that tetrahydroanabasine (5) was the substrate of the acetylation; however, the relevant nitrogen group of 5 is not a likely acetylation center due to weak nucleophilicity. Second, the apparent product of the acetylation, ammodendrine (6), has been ruled out as an intermediate in QA biosynthesis due to the absence of a particular hydrogen atom that must be retained during formation of the quinolizidine ring (11, 34). We surmount

both hurdles by proposing that the direct substrate of acetylation is not tetrahydroanabasine (5) but the carbinolamine 18 (fig. S9), which is likely in equilibrium with 5 under aqueous conditions (35–37). Accordingly, the direct product of the acetylation would be the carbinolamide 19, which does retain the mentioned hydrogen atom (fig. S9). In the revised hypothesis, 19 is the true downstream pathway intermediate, while ammodendrine (6) is formed spontaneously by dehydration in the absence of the subsequent pathway enzyme. It is worth mentioning that an acetylated QA, lusitanine (21), accumulates in several different lupin species (25). Its occurrence suggests that the acetyl group is retained at least past the formation of the quinolizidine ring. We summarize the revised pathway hypothesis in fig. S9, which can serve as a starting point for the discovery of the subsequent enzymes in the QA pathway, including a deacetylase responsible for removing the acetyl group.

AT is the first sweet gene to be unequivocally identified in lupins. Moreover, the discovery of the causal mutation (SNP_2) provides a mechanistic explanation for the process that enabled the modern domestication of white lupin. The creation of a non-GMO, sweet narrow-leaved lupin line by knocking out the orthologous gene demonstrates the potential to kick-start the domestication of novel legume crops via similar strategies. QAs accumulate not only in the cultivated lupin species but also in around 300 other

Lupinus species and most other legumes of the wider genistoid clade (38). Some of these could become excellent crop candidates upon genetic removal of QAs, for example, the forage legume tagasaste, also known as tree lucerne (*Cytisus proliferus*) (39). The use of non-GMO techniques as exemplified here is particularly attractive for legume crop candidates for which transformation protocols are not available and those that are grown in geopolitical areas with restrictive GMO legislation.

MATERIALS AND METHODS

LC-MS

LC-MS analyses were carried out on a Thermo Fisher Dionex 3000 RS HPLC/UPLC system interfaced to a Bruker compact QqTOF mass spectrometer through an electrospray ionization (ESI) source. ESI mass spectra (m/z 50 to 1000) were acquired in positive ionization mode with automatic MS² acquisition using the following parameters: capillary voltage of 4500 V, end plate offset of −500 V, source temperature of 250°C, desolvation gas flow of 8.0 liter/min, and nebulizer pressure of 2.5 bar. N₂ was used as desolvation, nebulizer, and collision cell gas.

LC method 1 (untargeted metabolite analysis in white lupin)

Analytes were separated on a Kinetex XB-C18 column (100 mm by 2.1 mm, 1.7 μ m, 100 Å, Phenomenex) kept at 40°C. Mobile phases A and B consisted of, respectively, 0.05% formic acid in water and 0.05% formic acid in acetonitrile. Analytes were eluted using the following gradient at a constant flow rate of 0.3 ml/min: 0 to 1 min, 2% B (constant); 1 to 16 min, 2 to 25% B (linear); 16 to 24 min, 25 to 65% B (linear); 24 to 26 min, 65 to 100% B (linear); 26 to 27 min, 100% B (constant); 27 to 27.5 min, 100 to 2% B (linear); and 27.5 to 33 min, 2% B (constant).

LC method 2 (QA quantification in narrow-leaved lupin *AT^{KO}* plants)

Analytes were separated on a Luna C18(2) column (150 mm by 2 mm, 3 μ m, 100 Å, Phenomenex) kept at 40°C. Mobile phases A and B consisted of, respectively, 0.05% formic acid in water and 0.05% formic acid in acetonitrile. Analytes were eluted using the following gradient at a constant flow rate of 0.3 ml/min: 0 to 0.5 min, 2% B (constant); 0.5 to 2.375 min, 2 to 6% B (linear); 2.375 to 7 min, 6 to 25% B (linear); 7 to 13 min, 25 to 100% B (linear); 13 to 14 min, 100% B (constant); 14 to 14.5 min, 100 to 2% B (linear); and 14.5 to 20 min, 2% B (constant).

Preparative high-performance LC

Preparative high-performance LC (HPLC) was carried out on a Shimadzu preparative HPLC system with ultraviolet detection (190 to 350 nm) and automatic fraction collection. The individual components of the system were: DGU-20A₅ degasser, SIL-10AP autosampler, LC-20AT pump, CTO-10ASvp column oven, SPD-M20A photodiode array detector, and FRC-10A fraction collector.

Analytes were separated on a Luna C18(2) semi-preparative column (250 mm by 10 mm, 5 μ m, 100 Å, Phenomenex) kept at 30°C. Mobile phases A and B consisted of, respectively, 0.05% formic acid in water and 0.05% formic acid in acetonitrile. Analytes were eluted using the following gradient at a constant flow rate of 2 ml/min: 0 to 2 min, 2% B (constant); 2 to 32 min, 2 to 25% B (linear); 32 to 37 min, 25 to 65% B (linear); 37 to 42 min, 65 to 95% B (linear); 42 to 45 min, 95% B (constant); 45 to 50 min, 95 to 5% B (linear); and 50 to 62 min, 2% B (linear). Ammodendrine

was collected in the fraction eluting between 21.82 and 22.41 min (λ_{max} = 240 nm).

Untargeted metabolite analysis of three white lupin accessions (P27174, Graecus, and Amiga)

Seedlings of white lupin accessions P27174 (n = 4), Graecus (n = 4), and Amiga (n = 5) were grown under hydroponic conditions as previously described (16). Young leaf material was first collected from the seedlings at the three true leaf stage. The same seedlings were then allowed to grow two more leaves (five true leaf stage). At this point, young leaf and stem material were also harvested. All samples were flash frozen in liquid nitrogen immediately after collection and stored at −50°C until further analysis.

The tissues were pulverized using a mortar and pestle chilled with liquid nitrogen. Five hundred microliters of extractant [60% methanol and 0.06% formic acid in water with caffeine (5 mg/liter) as internal standard] were added to 20 to 100 mg of frozen powder, and the mixtures were shaken vigorously for 2 hours at room temperature. After a brief centrifugation, the extracts were diluted five times with water, clarified through 0.22- μ m filters, and transferred to glass vials for LC-MS analysis using LC method 1 (2- μ l injections).

Each tissue sample was injected once, and a blank (extractant) and a quality control sample (extract pool) were included every 10th injection to ensure the absence of carryover and to monitor changes in sensitivity during the run. The raw LC-MS chromatograms were mass calibrated (sodium formate clusters), converted to mzXML format, and submitted to XCMS online (v.3.7.1) for peak alignment and metabolite feature detection and integration. The samples were then grouped by accession (P27174, Graecus, and Amiga) and processed together through a multi-job analysis using the default settings for UPLC/Bruker Q-TOF instruments. The parameters used for metabolite feature detection (centWave algorithm) were as follows: $\Delta m/z \leq 10$ parts per million (ppm), minimum peak width of 5 s, maximum peak width of 20 s, and signal-to-noise ratio > 5. A total of 6254 metabolite features were detected. Background metabolite features (those detected in the blanks) and those from the calibrant and re-equilibration segments (retention time < 0.5 min and > 27.5 min, respectively) were removed, leaving 3322 lupin metabolite features.

Only eight metabolite features were detected in 9 or more of the 15 tissue samples from Amiga but not in any of the samples from P27174 and Graecus. The eight features corresponded to 17 chromatographic peaks. The median m/z of the features was as follows: 199.1442 (two peaks), 201.1599 (one peak), 209.1649 (two features, four peaks), 262.1550 (two peaks), 287.0551 (two peaks), 321.6413 (one peak), and 343.1861 (five peaks). The MS² spectrum of all the peaks except those of m/z 287.0551 (probable flavonoids that were later also found in non-*pauper* accessions) contained a fragment with the mass of Δ^1 -piperidine (3) (m/z 84.08 \pm 0.01). The MS² spectrum of the peaks of m/z 343.1861 and m/z 321.6413 included also a fragment with the mass of tetrahydroanabasine (5) (m/z 167.16 \pm 0.01), dimer of Δ^1 -piperidine (3). The most intense of the Amiga-specific peaks were those associated with the features of m/z 209.1649, m/z 199.1442, and m/z 343.1861, in this order. These accumulated in sufficient amounts to be detected in all of the Amiga samples upon visual inspection of the chromatograms. Therefore, only these peaks (peaks b-l in Fig. 1C and fig. S1) were used as metabolic markers for *pauper* in our scoring of white lupin

accessions (see below). The compounds likely derive from the oxidation and conjugation of piperidine (3 or 4) and tetrahydroanabasine (5) in planta, but piperidine itself (3 or 4) was not detected in any of the samples. Instead, tetrahydroanabasine (5) (median m/z 167.1542) appeared as a single, broad peak in a fraction of the samples from Amiga (although in lower abundance compared to the others). The scaling factors for the m/z 167.15, 199.14, 209.16, and 343.19 extracted ion chromatograms in Fig. 1C and fig. S1 are, respectively, 10, 10, 1, and 10 (P27174 and Graecus); 15, 1, 2.5, and 15 (Amiga); and 3, 1, 40, and 15 (*N. benthamiana*).

Chemo- and genotyping of 150 individuals from 24 white lupin accessions

White lupin accessions were chosen from the Polish *Lupinus* collection to cover a wide range of seed alkaloid levels based on Kroc *et al.* (14). The chosen accessions represented different classes (wild forms, landraces, breeding lines, and cultivars) and different countries of origin. Plants were grown in the field at Poznan Plant Breeders Ltd., Wiatrowo, Poland (latitude, 52°45'9"N; longitude, 17°80'36"E; and altitude 86 m above sea level) during the growth seasons of 2016 and 2019. Fifteen seeds per accession were sown in rows during early spring (April), leaving 20 cm between seeds in a row and between rows. Fertilizers P₂O₅ and K₂O were applied at 60 and 90 kg/hectare, respectively, and weed control was carried out mechanically. Leaf samples were collected at flowering stage and immediately frozen for later chemo- and genotyping.

For AT genotyping, genomic DNA was extracted from 200 mg of frozen leaf tissue with the aid of the Maxwell RSC Instrument automatic nucleic acid purification platform and the Maxwell RSC Pure Food GMO and Authentication Kit (Promega). Polymerase chain reaction (PCR) was carried out on the extracted DNA using primers LalbAT_F1/R1 and LalbAT_F2/R2 (table S5), and the PCR products were subjected to Sanger sequencing.

For chemotyping, 20 to 70 mg of frozen leaf powder were extracted as described above for the untargeted metabolite analysis of Amiga, P27174, and Graecus and analyzed by LC-MS using LC method 1 (2- and 10- μ l injections). Lupanine content was measured using a known standard (Innosil), and the presence of the *pauper* metabolic markers of m/z 209.16, m/z 199.14, and m/z 343.19 (\pm 0.01) was scored by inspection of the corresponding extracted ion chromatograms (peak signal-to-noise ratio > 5). Samples were labeled as low QA (sweet) if they contained less than 0.02% of lupanine by frozen weight.

Chemo- and genotyping of 227 white lupin accessions

The white lupin accessions originated from 26 countries and included accessions from six Genebanks and two companies as well as newly collected accessions from Ethiopia. The seeds were chipped and germinated on agar before being vernalized at 4°C for 3 weeks. Seedlings were transferred to soil and grown in a glasshouse under long-day conditions. When plants had five and six true leaves, leaf material was collected for DNA extraction, and samples were tested for QAs by pressing freshly cut petioles onto filter paper soaked in Dragendorff reagent and observing the color change (40). DNA was extracted from young leaves using the DNeasy Plant Mini Kit (QIAGEN) and eluted into water. DNA was quantified using NanoDrop and Qubit assays (Thermo Fisher Scientific), and samples were normalized to 50 ng/ μ l. Purified DNA samples were provided

to LGC Genomics (Berlin, Germany) for genotyping by sequencing using SeqSNP, including technical replicate samples for Kiev mutant and P27174. Among the 10,000 SNP targets in the SeqSNP genotyping set were 16 SNPs in the *AT* gene (Chr18g0051511). SeqSNP results are only reported for the four relevant SNPs (see Fig. 2A).

Chemo- and genotyping of conflicting white lupin accessions

Seed samples of three white lupin accessions were retrieved from the Polish *Lupinus* collection: 95015 (San Felices), 95023 (Oeiras-930/3), and 95064 (Population-8062). For each accession, 10 seeds were sown in the experimental field at the Institute of Plant Genetics, Polish Academy of Sciences, Poznan, Poland (latitude, 52°26'48"N; longitude, 16°54'11"E). Leaf and seed material of all germinated plants underwent genotyping and chemotyping. Genotyping was performed as described above for the chemo- and genotyping of 150 individuals from 24 white lupin accessions. For chemotyping, the total alkaloid content of the mature, dry seeds was determined by GC-FID as previously described (41).

Pathway reconstruction by transient coexpression in *N. benthamiana*

Total RNA was extracted from young leaves of narrow-leaved lupin cv. Oskar and white lupin accession P27174 using the Spectrum Plant Total RNA Kit (Sigma-Aldrich). cDNA was synthesized using the iScript cDNA Synthesis Kit (Bio-Rad). Full-length coding sequences of *LDC* [National Center for Biotechnology Information (NCBI) GenBank AB560664], *CAO* (NCBI GenBank MF152953), and *AT* (DNA Sequence 1 in the Supplementary Materials) were amplified from lupin leaf cDNA (primers in table S5) and cloned into the plant expression vector pEAQ-USER (42) by USER cloning (43). The constructs were transformed into *Agrobacterium tumefaciens* strain AGL-1. The AGL-1 strains were cultured in 1% yeast extract, 1% peptone medium supplemented with kanamycin (50 μ g/ml), rifampicin (25 μ g/ml), and carbenicillin (50 μ g/ml) at 28°C and 220 rpm to optical density at 600 nm (OD_{600}) \times 3. The presence of the desired pEAQ-USER construct was confirmed by culture PCR. Following a brief centrifugation, bacterial pellets were resuspended in water to OD_{600} = 1. After a 1- to 3-hour incubation at room temperature, the bacterial suspensions were infiltrated into the abaxial side of the young leaves of 4- to 5-week-old *N. benthamiana* plants using a 3-ml syringe without a needle. To coexpress multiple genes in the same leaf, suspensions of the corresponding AGL-1 strains were mixed in equal volumes before the infiltration. Only the youngest, fully expanded leaf of each plant was infiltrated, and three to five plants were used for each combination of genes.

Agroinfiltrated leaves were harvested 9 days after infiltration. Two 1-cm leaf discs were punched out of the infiltrated (slightly discolored) portion of the leaves and flash-frozen in liquid nitrogen. The discs were pulverized using steel balls and a TissueLyser II bead beater (QIAGEN). The pulverized leaf discs were extracted with 250 μ l of extractant [60% methanol and 0.06% formic acid in water with caffeine (5 mg/liter) as internal standard] by vigorously shaking for 2 hours at room temperature. The solids were separated by centrifugation, and the supernatants were diluted 5 \times with water, passed through 0.22- μ m filters, and transferred to glass vials for LC-MS analysis using LC method 1.

Purification and structural elucidation of the AT product from *N. benthamiana*

LDC, CAO, and AT were coexpressed in young leaves from 4-week-old *N. benthamiana* plants by agroinfiltration as described above. Whole infiltrated leaves were harvested 7 days after the agroinfiltration, quickly frozen in liquid nitrogen, and pulverized. A total of 5 ml of extractant (60% methanol and 0.06% formic acid in water) were added to 800 mg of frozen leaf powder. The mixture was shaken for 2 hours at room temperature. The light green mixture was centrifuged, and the supernatant was concentrated under vacuum at room temperature to a viscous yellow oil. The oily residue was diluted with 2 ml of 20% methanol in water and passed through a 0.22- μ m filter.

Ammodendrine was isolated from the extracts as its formate salt by preparative HPLC (200- μ l injections). The ammodendrine fractions from up to 40 consecutive injections were pooled and dried at 35°C under vacuum to a white, powdery residue. The residue was dissolved in D₂O with 0.05% sodium 2,2-dimethyl-2-silapentane-5-sulfonate (DSS) as internal reference (calibrated to δ_{H} 0.0 ppm and δ_{C} 0.0 ppm) and analyzed by NMR spectroscopy. NMR spectra were acquired at 300 K on a Bruker Avance III spectrometer (¹H operating frequency of 600.13 MHz) equipped with a Bruker SampleJet sample changer and a cryogenically cooled gradient inverse triple resonance 1.7-mm TCI probe-head (Bruker Biospin, Karlsruhe, Germany) using standard one-dimensional (1D) and 2D experiments [¹³C NMR data were assigned using heteronuclear single quantum coherence (HSQC) and heteronuclear multiple bond correlation (HMBC) experiments]. Data were processed using TopSpin version 4.1.4 (Bruker). Ammodendrine (**6**) appeared as an equimolar mixture of *cis:trans* rotamers about the amide bond in D₂O.

cis-Ammodendrine

¹H NMR (600 MHz, D₂O, 300 K, DSS): δ_{H} 6.90 (1H, s, H6), 3.67 (1H, m, H2'ax), 3.63 (1H, m, H2A), 3.52 (1H, ddd, *J* = 13.0, 7.7, 3.7 Hz, H2B), 3.41 (1H, d, *J* = 11.4 Hz, H6'eq), 3.06 (1H, t, *J* = 12 Hz, 6'ax), 2.20 (3H, s, H8), 2.18 (1H, m, H4A), 2.10 (1H, m, H4B), 1.94 (1H, m, H4'eq), 1.92 (1H, m, H3'eq), 1.89 (1H, m, H5'eq), 1.86 (2H, m, H3), 1.78 (1H, m, H3'ax), 1.65 (1H, m, H5'ax), and 1.58 (1H, m, H4'ax). ¹³C NMR (150 MHz, D₂O, 300 K, DSS): δ_{C} 174.9 (C7), 128.8 (C6), 120.3 (C5), 63.7 (C2'), 47.9 (C6'), 43.0 (C2), 30.1 (C3'), 24.7 (C4'), 24.3 (C5'), 23.8 (C4), 23.3 (C8), and 23.1 (C3).

trans-Ammodendrine

¹H NMR (600 MHz, D₂O, 300 K, DSS): δ_{H} 7.23 (1H, s, H6), 3.69 (1H, m, H2'ax), 3.66 (1H, m, H2A), 3.59 (1H, m, H2B), 3.41 (1H, d, *J* = 11.4 Hz, H6'eq), 3.06 (1H, t, *J* = 12 Hz, H6'ax), 2.19 (3H, s, H8), 2.18 (1H, m, H4A), 2.10 (1H, m, H4B), 1.94 (1H, m, H4'eq), 1.92 (1H, m, H3'eq), 1.92 (2H, m, H3), 1.89 (1H, m, H5'eq), 1.78 (1H, m, H3'ax), 1.65 (1H, m, H5'ax), and 1.58 (1H, m, H4'ax). ¹³C NMR (150 MHz, D₂O, 300 K, DSS): δ_{C} 174.9 (C7), 125.9 (C6), 121.7 (C5), 63.7 (C2'), 47.9 (C6'), 46.9 (C2), 30.1 (C3'), 24.7 (C4'), 24.3 (C5'), 23.9 (C4), 23.7 (C8), and 23.6 (C3).

High-resolution mass of [M+H]⁺ calculated for C₁₂H₂₁N₂O: 209.1648; found 209.1649 (err. −0.3 ppm).

Chemical synthesis of α -tripiperideine and tetrahydroanabasine

The two different trimers of Δ^1 -piperideine (**3**), α -tripiperideine and isotripiperideine, were synthesized as previously described (44). Tetrahydroanabasine was prepared as the hydrobromide salt

of its carbinolamine form using isotripiperdiene as a starting point, as previously described (37).

Heterologous protein expression, purification, and assays

Full-length sequences of the AT versions from accessions Amiga and P27174 were codon-optimized for expression in *E. coli* (see DNA Sequences 4 and 5 in the Supplementary Materials). The codon-optimized sequences were synthesized and cloned between the Nde I and Xho I restriction sites of the expression vector pET28a(+) by Twist Bioscience. However, N-terminally His-tagged AT proved to be insoluble when expressed in *E. coli* in our initial tests. To increase solubility, the enzyme was fused to the common solubility tag, *E. coli* MBP. A custom T7-lac-based expression cassette was designed to encode a cleavable (by HRV 3C protease), N-terminally His-tagged MBP tag upstream of a USER cloning site (fig. S8A and DNA Sequence 6 in the Supplementary Materials). The cassette was synthesized and cloned between the Bgl II and Xho I restriction sites of expression vector pET24a(+) by Twist Bioscience. The resulting new plasmid (pET24-HMP-USER) was amplified in *E. coli* strain TOP10 and digested with Pac I and Nt.BbvC I. The codon-optimized AT versions from Amiga and P27174 were then cloned by USER cloning (43) in frame with the N-terminal tags using the primers specified in table S5. The point mutations leading to the Amiga^{E35D} and P27174^{D35E} AT versions were introduced in the respective codon-optimized sequences via USER fusion (45) using an additional primer pair carrying the desired mutation for each version (table S5).

The four AT constructs in pET24-HMP-USER were transformed into *E. coli* strain ArcticExpress (DE3) RIL. The ArcticExpress strains were precultured overnight at 37°C and 220 rpm in selective LB [gentamicin (20 μ g/ml), streptomycin (75 μ g/ml), tetracycline (10 μ g/ml), and kanamycin (50 μ g/ml)] from fresh, single colonies. A 2-ml aliquot of preculture was added to 100 ml of terrific broth [yeast extract (24 g/liter), tryptone (20 g/liter), glycerol (4 ml/liter), 17 mM KH₂PO₄, and 72 mM K₂HPO₄ (pH 7.2)] without antibiotics and incubated at 30°C and 220 rpm to OD₆₀₀ \approx 0.6 to 0.8. The cultures were briefly cooled down in an ice-water bath, and the AT expression was induced with 0.250 mM isopropyl- β -D-thiogalactopyranoside (IPTG). The cultures were incubated at 10°C and 220 rpm for 60 to 90 hours after which bacterial pellets were resuspended in 6 ml of ice-cold lysis buffer [300 mM NaCl, 10% glycerol, 50 mM Na₂HPO₄, and lysozyme (100 μ g/ml) (pH 8.0)]. The cells were lysed by sonication on ice-water, and the lysates were cleared by centrifugation at 4°C and 20,000 rcf for 20 min. For affinity purification, the cleared lysates were incubated with 1.5 ml of 50% Ni-NTA agarose resin (QIAGEN) for 1 hour at 4°C on a tube rotator. The matrix was washed with 12 ml of ice-cold wash buffer [300 mM NaCl, 10% glycerol, 50 mM Na₂HPO₄, and 25 mM Imidazole (pH 8.0)]. Bound proteins were eluted with 4.5 ml of ice-cold elution buffer [300 mM NaCl, 10% glycerol, 50 mM Na₂HPO₄, and 500 mM imidazole (pH 8.0)]. Imidazole was removed via Amicon Ultra MWCO 30 kDa diafiltration centrifugal columns (Merck), which also served to concentrate the protein 90 \times using exchange buffer [300 mM NaCl, 10% glycerol, and 50 mM Na₂HPO₄ (pH 8.0)]. The final concentration of tagged AT was determined by in-gel quantification using Criterion TGX strain free gels (Bio-Rad) and a bovine serum albumin (BSA) standard (Bio-Rad). The protein preparations could be stored at 4°C

for up to 15 days with ~50% loss in activity. See also Extended Methods in Supplementary Materials.

To measure the rate of the acetylation reactions, we developed an absorption-based assay in microtiter plate format. In the assay, co-enzyme A produced by AT reacted quantitatively and in real time with the thiol scavenger and chromogen 5,5'-dithiobis(2-nitrobenzoic acid) (DTNB) to form a yellow compound ($\lambda_{\text{max}} = 412 \text{ nm}$). Individual reactions were carried out in a final volume of 200 μl and contained 100 mM Na_2HPO_4 (pH 8.0), 500 μM DTNB (Sigma-Aldrich), 1 mM acetyl-coenzyme A trilithium salt (Roche), 1 mM Δ^1 -piperidine (prepared in house from α -tripiperidine; see Extended Methods in the Supplementary Materials), and 5 to 50 μg of tagged AT. In alternative assays, the Δ^1 -piperidine was replaced by 0.5 mM tetrahydroanabasine dihydrobromide. Care was taken not to mix AT with acetyl-coenzyme A and DTNB before the start of the assay, as doing so appeared to inhibit the enzyme. Assays were started by adding 195 μl of a mixture of substrates and DTNB to 5- μl aliquots of the protein, and absorbance at 412 nm was monitored for 10 min at room temperature using a microplate reader with 3-s shaking between each reading. See Extended Methods for additional details.

Narrow-leaved lupin mutant library construction

The narrow-leaved lupin mutant library was constructed essentially as described in Knudsen *et al.* (30). Briefly, 15 kg of narrow-leaved lupin cultivar Oskar was subjected to mutagenesis using 0.1% EMS for 16 hours at 23°C. The EMS was removed by three successive washes with water before the seeds were fan dried on filter paper in a fume hood. The dried M1 seeds were subsequently shipped to New Zealand for field propagation and harvest. Plants were harvested in 5- m^2 pools using a combine harvester. Genomic DNA was extracted from subsamples of each pool of M2 seeds, and the remaining pool was stored until seed extraction.

Isolation and characterization of a narrow-leaved lupin AT knockout

The narrow-leaved lupin mutant library was screened essentially as described in Knudsen *et al.* (30). Briefly, a TaqMan assay was designed to identify a specific base change at position 506 in the coding region of AT, which corresponds to the change in amino acid 169 from tryptophan to a premature stop (see DNA Sequence 7 in the Supplementary Materials). For the TaqMan assay, we designed a target-specific forward primer (AT_TaqMan_FW), a target-specific reverse primer (AT_TaqMan_RV), a wild-type-specific probe containing both a HEX fluorophore and a BHQ1 quencher (ATWT_TaqMan_HEX), and a mutant-specific probe containing both the FAM fluorophore and a BHQ1 quencher (ATKO_TaqMan_FAM). The TaqMan assay was used to screen the pools of the narrow-leaved lupin mutant DNA library utilizing the FIND-IT workflow (30). Subsequently, one individual heterozygous mutant seed was extracted from a positive pool of the library by subjecting 768 individual seeds to a nondestructive DNA extraction procedure as described previously for barley (30).

The M2 heterozygous mutant plant that grew from the seed was allowed to self-pollinate. The resulting M3 seeds were sown in 16-cm-wide, 20-cm-deep pots filled with commercial peat-based potting soil and grown in a growth cabinet with a light/dark photoperiod of 16/8 hours at day/night temperatures of 21°/18°C and at 60% relative humidity. Young leaves from the M3 plants were dried

for 12 hours at 50°C and pulverized using steel balls and a bead beater. Genomic DNA was extracted from ~5 mg of dry leaf powder using the E.Z.N.A. Plant DNA DS Kit (Omega Bio-tek), and the plants were subsequently genotyped by sequencing a 315-bp-long PCR fragment spanning the early stop codon using primers ATKO_GnTp_FW and ATKO_GnTp_RV. QAs were extracted from ~10 mg of dry leaf powder with 1 ml of extractant (60% methanol and 0.06% formic acid in water with 15-ppm caffeine as internal standard) by mixing vigorously for 2.5 hours at room temperature. The extracts were clarified by centrifugation, diluted 15 \times with water, and filtered through a 0.22- μm filter. The samples were analyzed by LC-MS using LC method 2 (1- μl injections). The identity of the alkaloids was inferred from their *m/z* and MS² fragmentation spectrum (22). For relative quantification, QA peak areas were normalized by the area of the caffeine peak and by the weight of the sample ($n = 6$ for each genotype). The total alkaloid content of the mature, dry seeds of the M3 plants was determined by GC-FID as previously described (41).

Supplementary Materials

This PDF file includes:

Extended Methods
DNA Sequences 1 to 7
Figs. S1 to S9
Legends for tables S1 to S5
References

Other Supplementary Material for this

manuscript includes the following:

Tables S1 to S5

REFERENCES AND NOTES

1. World Health Organization, Regional Office for Europe, "Plant-based diets and their impact on health, sustainability and the environment: A review of the evidence" (World Health Organization, 2021).
2. A. Boerema, A. Peeters, S. Swolfs, F. Vandevenne, S. Jacobs, J. Staes, P. Meire, Soybean Trade: Balancing environmental and socio-economic impacts of an intercontinental market. *PLOS ONE* **11**, e0155222 (2016).
3. M. M. Lucas, F. Stoddard, P. Annicchiarico, J. Frias, C. Martinez-Villaluenga, D. Sussmann, M. Duranti, A. Seger, P. Zander, J. Pueyo, The future of lupin as a protein crop in Europe. *Front. Plant Sci.* **6**, 705 (2015).
4. K. M. Frick, L. G. Kamphuis, K. H. M. Siddique, K. B. Singh, R. C. Foley, Quinolizidine alkaloid biosynthesis in lupins and prospects for grain quality improvement. *Front. Plant Sci.* **8**, 87 (2017).
5. R. von Sengbusch, Süßlupinen und Öllupinen, Die Entstehungsgeschichte einiger neuer Kulturpflanzen. *Landw. Jahrb.* **91**, 793–880 (1942).
6. W. A. Cowling, J. S. Gladstones, Lupin breeding in Australia, in *Linking Research and Marketing Opportunities for Pulses in the 21st Century: Proceedings of the Third International Food Legumes Research Conference*, R. Knight, Ed. (Springer Netherlands, 2000), pp. 541–547.
7. J. S. Gladstones, Distribution, origin, taxonomy, history and importance, in *Lupinus as Crop Plants: Biology, Production and Utilization*, J. S. Gladstones, C. Atkins, J. Hamblin, Eds. (CAB International, 1998), pp. 1–37.
8. J. C. Clements, W. A. Cowling, Patterns of morphological diversity in relation to geographical origins of wild *Lupinus angustifolius* from the Aegean region. *Genet. Resour. Crop Evol.* **41**, 109–122 (1994).
9. L. Yeheyis, W. Mekonnen, M. Nelson, D. Mcnaughton, A. Tarekegn, Z. Yadelew, H. Sanders, The search for commercial sweet white lupin (*Lupinus albus* L.) adaptive to Ethiopian growing condition seems not successful: What should be done? *Z. Naturforsch. C* **78**, 317–325 (2023). <https://doi.org/10.1515/znc-2023-0033>.
10. S. L. Otterbach, T. Yang, L. Kato, C. Janfelt, F. Geu-Flores, Quinolizidine alkaloids are transported to seeds of bitter narrow-leaved lupin. *J. Exp. Bot.* **70**, 5799–5808 (2019).

11. D. Mancinotti, K. M. Frick, F. Geu-Flores, Biosynthesis of quinolizidine alkaloids in lupins: mechanistic considerations and prospects for pathway elucidation. *Nat. Prod. Rep.* **39**, 1423–1437 (2022).
12. S. Bunsupa, K. Katayama, E. Ikeura, A. Oikawa, K. Toyooka, K. Saito, M. Yamazaki, Lysine decarboxylase catalyzes the first step of quinolizidine alkaloid biosynthesis and coevolved with alkaloid production in leguminosae. *Plant Cell* **24**, 1202–1216 (2012).
13. T. Yang, I. Nagy, D. Mancinotti, S. L. Otterbach, T. B. Andersen, M. S. Motawia, T. Asp, F. Geu-Flores, Transcript profiling of a bitter variety of narrow-leaved lupin to discover alkaloid biosynthetic genes. *J. Exp. Bot.* **68**, 5527–5537 (2017).
14. M. Kroc, W. Rybiński, P. Wilczura, K. Kamel, Z. Kaczmarek, P. Barzyk, W. Świąćicki, Quantitative and qualitative analysis of alkaloids composition in the seeds of a white lupin (*Lupinus albus* L.) collection. *Genet. Resour. Crop Evol.* **64**, 1853–1860 (2017).
15. R. Lin, D. Renshaw, D. Luckett, J. Clements, G. Yan, K. Adhikari, B. Buirchell, M. Sweetingham, H. Yang, Development of a sequence-specific PCR marker linked to the gene “pauper” conferring low-alkaloids in white lupin (*Lupinus albus* L.) for marker assisted selection. *Mol. Breed.* **23**, 153–161 (2009).
16. B. Hufnagel, A. Marques, A. Soriano, L. Marquès, F. Divol, P. Dumas, E. Sallet, D. Mancinotti, S. Carrere, W. Marande, S. Arribat, J. Keller, C. Huneau, T. Blein, D. Aimé, M. Laguerre, J. Taylor, V. Schubert, M. Nelson, F. Geu-Flores, M. Crespi, K. Gallardo, P.-M. Delaux, J. Salse, H. Bergès, R. Guyot, J. Gouzy, B. Péret, High-quality genome sequence of white lupin provides insight into soil exploration and seed quality. *Nat. Commun.* **11**, 492 (2020).
17. M. Książkiewicz, N. Nazzicari, H. Yang, M. N. Nelson, D. Renshaw, S. Rychel, B. Ferrari, M. Carelli, M. Tomaszewska, S. Stawiński, B. Naganowska, B. Wolko, P. Annicchiarico, A high-density consensus linkage map of white lupin highlights synteny with narrow-leaved lupin and provides markers tagging key agronomic traits. *Sci. Rep.* **7**, 15335 (2017).
18. S. Rychel, M. Książkiewicz, Development of gene-based molecular markers tagging low alkaloid pauper locus in white lupin (*Lupinus albus* L.). *J. Appl. Genet.* **60**, 269–281 (2019).
19. B. Hufnagel, A. Soriano, J. Taylor, F. Divol, M. Kroc, H. Sanders, L. Yeheyis, M. Nelson, B. Péret, Pangenome of white lupin provides insights into the diversity of the species. *Plant Biotechnol. J.* **19**, 2532–2543 (2021).
20. I. Zafeiriou, A. N. Polidoros, E. Baira, K. M. Kasiotis, K. Machera, P. V. Mylona, Mediterranean white lupin landraces as a valuable genetic reserve for breeding. *Plants* **10**, 2403 (2021).
21. S. Bunsupa, T. Okada, K. Saito, M. Yamazaki, An acyltransferase-like gene obtained by differential gene expression profiles of quinolizidine alkaloid-producing and nonproducing cultivars of *Lupinus angustifolius*. *Plant Biotechnol.* **28**, 89–94 (2011).
22. D. Mancinotti, M. C. Rodríguez, K. M. Frick, B. Dueholm, D. G. Jepsen, N. Agerbirk, F. Geu-Flores, Development and application of a virus-induced gene silencing protocol for the study of gene function in narrow-leaved lupin. *Plant Methods* **17**, 131 (2021).
23. K. Czepiel, P. Krajewski, P. Wilczura, P. Bielecka, W. Świąćicki, M. Kroc, Expression profiles of alkaloid-related genes across the organs of narrow-leaved lupin (*Lupinus angustifolius* L.) and in response to anthracnose infection. *Int. J. Mol. Sci.* **22**, 2676 (2021).
24. A. M. Brown, D. J. Robins, L. Witte, M. Wink, Stereochemistry of enzymic reactions involved in the formation of tetrahydroanabasine, ammodendrine, spimpine, and tripiperidine. *Life Sci. Adv.* **10**, 179–185 (1991).
25. M. Wink, C. Meißner, L. Witte, Patterns of quinolizidine alkaloids in 56 species of the genus *Lupinus*. *Phytochemistry* **38**, 139–153 (1995).
26. T.-T. T. Dang, X. Chen, P. J. Facchini, Acetylation serves as a protective group in noscapine biosynthesis in opium poppy. *Nat. Chem. Biol.* **11**, 104–106 (2015).
27. L. Caputi, J. Franke, S. C. Farrow, K. Chung, R. M. E. Payne, T.-D. Nguyen, T.-T. T. Dang, I. S. T. Carqueijeiro, K. Koudounas, T. D. de Bernonville, B. Ameyaw, D. M. Jones, I. J. C. Vieira, V. Courdavaud, S. E. O’Connor, Missing enzymes in the biosynthesis of the anticancer drug vinblastine in Madagascar periwinkle. *Science* **360**, 1235–1239 (2018).
28. Y. Qu, M. E. A. M. Easson, R. Simionescu, J. Hajicek, A. M. K. Thamm, V. Salim, V. De Luca, Solution of the multistep pathway for assembly of corynanthean, strychnos, iboga, and aspidosperma monoterpenoid indole alkaloids from 19E-geissoschizine. *Proc. Natl. Acad. Sci. U.S.A.* **115**, 3180–3185 (2018).
29. A. Bayer, X. Ma, J. Stöckigt, Acetyltransfer in natural product biosynthesis—Functional cloning and molecular analysis of vinorine synthase. *Biorg. Med. Chem.* **12**, 2787–2795 (2004).
30. S. Knudsen, T. Wendt, C. Dockter, H. C. Thomsen, M. Rasmussen, M. Egevang Jørgensen, Q. Lu, C. Voss, E. Murozuka, J. T. Østerberg, J. Harholt, I. Braumann, J. A. Cuesta-Seijo, S. M. Kale, S. Bodevin, L. Tang Petersen, M. Carciofi, P. R. Pedas, J. Opstrup Husum, M. T. S. Nielsen, K. Nielsen, M. K. Jensen, L. A. Møller, Z. Gojkovic, A. Striebeck, K. Lengeler, R. T. Fennessy, M. Katz, R. Garcia Sanchez, N. Solodovnikova, J. Förster, O. Olsen, B. L. Møller, G. B. Fincher, B. Skadhauge, FIND-IT: Accelerated trait development for a green evolution. *Sci. Adv.* **8**, eabq2266 (2022).
31. M. Kroc, G. Koczyk, K. A. Kamel, K. Czepiel, O. Fedorowicz-Strońska, P. Krajewski, J. Kosińska, J. Podkościwni, P. Wilczura, W. Świąćicki, Transcriptome-derived investigation of biosynthesis of quinolizidine alkaloids in narrow-leaved lupin (*Lupinus angustifolius* L.) highlights candidate genes linked to *iucundus* locus. *Sci. Rep.* **9**, 2231 (2019).
32. M. Kroc, K. Czepiel, P. Wilczura, M. Mokrzycka, W. Świąćicki, Development and validation of a gene-targeted dCAPS marker for marker-assisted selection of low-alkaloid content in seeds of narrow-leaved lupin (*Lupinus angustifolius* L.). *Genes* **10**, 428 (2019).
33. K. A. Kamel, W. Świąćicki, Z. Kaczmarek, P. Barzyk, Quantitative and qualitative content of alkaloids in seeds of a narrow-leaved lupin (*Lupinus angustifolius* L.) collection. *Genet. Resour. Crop Evol.* **63**, 711–719 (2016).
34. D. J. Robins, G. N. Sheldrake, Stereochemistry of quinolizidine alkaloid biosynthesis: Incorporation of the enantiomeric [2-²H]cadaverines into lupinine. *J. Chem. Soc. Chem. Commun.*, 1331–1332 (1994).
35. E. H. Cordes, W. P. Jencks, On the mechanism of schiff base formation and hydrolysis. *J. Am. Chem. Soc.* **84**, 832–837 (1962).
36. C. Struve, C. Christophersen, Structural equilibrium and ring-chain tautomerism of aqueous solutions of 4-aminobutyraldehyde. *Heterocycles* **60**, 1907–1914 (2003).
37. C. Schöpf, F. Braun, H. Koop, G. Werner, H. Bressler, K. Neisius, E. Schmadel, Über kristallisierte Salze des Δ¹-Tetrahydroanabasins und die absolute Konfiguration des (+)- bzw. (–)-α,β-Dipiperidyls. *Justus Liebigs Ann. Chem.* **658**, 156–168 (1962).
38. S. Ohmiya, K. Saito, I. Murakoshi, in *The Alkaloids: Chemistry and Pharmacology*, G. A. Cordell, Ed. (Academic Press, 1995), vol. 47, pp. 1–114.
39. M. R. Ventura, J. L. R. Castanon, M. Muzquiz, P. Mendez, M. P. Flores, Influence of alkaloid content on intake of subspecies of *Chamaecytisus proliferus*. *Anim. Feed Sci. Technol.* **85**, 279–282 (2000).
40. S. L. Noffsinger, E. van Santen, Evaluation of *Lupinus albus* L. Germplasm for the South-eastern USA. *Crop Sci.* **45**, 1941–1950 (2005).
41. W. Świąćicki, K. Czepiel, P. Wilczura, P. Barzyk, Z. Kaczmarek, M. Kroc, Chromatographic fingerprinting of the old world lupins seed alkaloids: A supplemental tool in species Discrimination. *Plants* **8**, 548 (2019).
42. D. Luo, R. Callari, B. Hamberger, S. G. Wubshet, M. T. Nielsen, J. Andersen-Ranberg, B. M. Hallström, F. Cozzi, H. Heider, B. Lindberg Møller, D. Staerk, B. Hamberger, Oxidation and cyclization of casbene in the biosynthesis of Euphorbia factors from mature seeds of *Euphorbia lathyris* L. *Proc. Natl. Acad. Sci. U.S.A.* **113**, E5082–E5089 (2016).
43. H. H. Nour-Eldin, F. Geu-Flores, B. A. Halkier, USER cloning and USER fusion: The ideal cloning techniques for small and big laboratories, in *Plant Secondary Metabolism Engineering: Methods and Applications*, A. G. Fett-Neto, Ed. (Humana Press, 2010), pp. 185–200.
44. A. Rouchaud, J.-C. Braekman, Synthesis of New Analogues of the Tetraonerines. *Eur. J. Org. Chem.* **2009**, 2666–2674 (2009).
45. F. Geu-Flores, H. H. Nour-Eldin, M. T. Nielsen, B. A. Halkier, USER fusion: A rapid and efficient method for simultaneous fusion and cloning of multiple PCR products. *Nucleic Acids Res.* **35**, e55 (2007).
46. J. S. Gladstones, Lupins as crop plants. *Field Crop Abstr.* **23**, 123–148 (1970).
47. J. Hackbarth, Die Gene der Lupinenarten. III Weiße Lupine (*Lupinus albus*). *Z. Pflanzenzüchtg.* **37**, 185–191 (1957).
48. J. E. M. Harrison, W. Williams, Genetical control of alkaloids in *Lupinus albus*. *Euphytica* **31**, 357–364 (1982).

Acknowledgments: We thank industry partner H. Sanders for the leadership role in Innovate UK project 133048. **Funding:** This work was supported by the VILLUM Foundation project 15476 (D.M., H.G.G., and F.G.-F.), the Novo Nordisk Foundation project NNF2019OC53580 (D.M., H.G.G., and F.G.-F.), the Polish Ministry of Agriculture and Rural Development Multiannual Programme RM-111-222-15 (K.C. and M.K.), Innovate UK project 133048 (J.L.T., L.Y., and M.N.N.), and the European Research Council (ERC) under the European Union's Horizon 2020 research and innovation program Starting Grant LUPINROOTS grant agreement no. 637420 (B.H. and B.P.). **Author contributions:** F.G.-F., D.M., M.K., K.C., M.N.N., J.L.T., B.P., and B.H. conceived the project. D.M., K.C., J.L.T., H.G.G., L.A.M., M.K.J., M.S.M., B.H., A.S., and L.K. carried out the experiments and data analysis. B.H., L.Y., T.W., and D.S. provided instrumentation, resources, and supervision. F.G.-F., M.K., M.N.N., and B.P. acquired the funding. F.G.-F. coordinated the project. D.M. prepared the figures. D.M. and F.G.-F. wrote the manuscript with input from all authors. **Competing interests:** The FIND-IT methodology presented in the manuscript is applied commercially by Traitomic A/S (www.traitomic.com), to which L.A.M., M.K.J., and T.W. are affiliated. The other authors declare no competing interests. **Data and materials availability:** All data needed to evaluate the conclusions in the paper are present in the paper and the Supplementary Materials. Seeds of the narrow-leaved lupin AT knockout can be provided by the University of Copenhagen pending scientific review and a completed material transfer agreement. Requests should be submitted to F.G.-F.

Submitted 27 January 2023
Accepted 5 July 2023
Published 4 August 2023
10.1126/sciadv.adg8866